The Prostate 77:654–671 (2017)

LuCaP Prostate Cancer Patient-Derived Xenografts Reflect the Molecular Heterogeneity of Advanced Disease and Serve as Models for Evaluating Cancer Therapeutics

Holly M. Nguyen,[1] Robert L. Vessella,[1,2] Colm Morrissey,[1] Lisha G. Brown,[1] Ilsa M. Coleman,[3] Celestia S. Higano,[4,5] Elahe A. Mostaghel,[4] Xiaotun Zhang,[1] Lawrence D. True,[6] Hung-Ming Lam,[1] Martine Roudier,[1] Paul H. Lange,[1] Peter S. Nelson,[1,3,6] and Eva Corey[1]*

[1]*Department of Urology, University of Washington, Seattle, Washington*
[2]*Puget Sound Veteran Administration, Seattle, Washington*
[3]*Division of Human Biology, Fred Hutchinson Cancer Research Center, Seattle, Washington*
[4]*Division of Clinical Research, Fred Hutchinson Cancer Research Center, Seattle, Washington*
[5]*Division of Oncology, Department of Medicine, University of Washington, Seattle, Washington*
[6]*Department of Pathology, University of Washington, Seattle, Washington*

BACKGROUND. Metastatic prostate cancer is a common and lethal disease for which there are no therapies that produce cures or long-term durable remissions. Clinically relevant preclinical models are needed to increase our understanding of biology of this malignancy and to evaluate new agents that might provide effective treatment. Our objective was to establish and characterize patient-derived xenografts (PDXs) from advanced prostate cancer (PC) for investigation of biology and evaluation of new treatment modalities.

METHODS. Samples of advanced PC obtained from primary prostate cancer obtained at surgery or from metastases collected at time of death were implanted into immunocompromised mice to establish PDXs. Established PDXs were propagated in vivo. Genomic, transcriptomic, and STR profiles were generated. Responses to androgen deprivation and docetaxel in vivo were characterized.

RESULTS. We established multiple PDXs (LuCaP series), which represent the major genomic and phenotypic features of the disease in humans, including amplification of androgen receptor, *PTEN* deletion, *TP53* deletion and mutation, *RB1* loss, TMPRSS2-ERG rearrangements, *SPOP* mutation, hypermutation due to MSH2/MSH6 genomic aberrations, and *BRCA2* loss. The PDX models also exhibit variation in intra-tumoral androgen levels. Our in vivo results show heterogeneity of response to androgen deprivation and

Grant sponsor: Richard M. Lucas Foundation; Grant sponsor: Prostate Cancer Foundation; Grant sponsor: NIH; Grant number: PO1 CA163227; Grant sponsor: PNW Prostate Cancer SPORE NIH; Grant numbers: P50 CA097186; 1R01CA165573; R21 CA194798; Grant sponsor: Department of Defense Prostate Cancer Research Program; Grant numbers: W81XWH-14-2-0183; W81XWH-15-1-0562; W81XWH-15-1-0430; Grant sponsor: FHCRC/UW Cancer Consortium; Grant number: P30CA15704; Grant sponsor: Institute of Prostate Cancer Research; Grant sponsor: a Stand Up To Cancer-Prostate Cancer Foundation Prostate Dream Team Translational Cancer Research; Grant number: SU2C-AACR-DT0712.

Current institution of Xiaotun Zhang is Pathology, Mayo Clinic, Rochester, MI, USA.

Current Institution of Martine Roudier is AstraZeneca, Pathology, Translational Oncology, Cambridge, UK.

Holly M. Nguyen and Robert L. Vessella are the co-primary lead authors.

Conflicts of interest: The authors declare no potential conflicts of interest.

*Correspondence to: Eva Corey, Department of Urology, Mailstop 356510, University of Washington, Seattle, WA 98195.
E-mail: ecorey@uw.edu
Received 22 December 2016; Accepted 6 January 2017
DOI 10.1002/pros.23313
Published online 3 February 2017 in Wiley Online Library (wileyonlinelibrary.com).

docetaxel, standard therapies for advanced PC, similar to the responses of patients to these treatments.

CONCLUSIONS. The LuCaP PDX series reflects the diverse molecular composition of human castration-resistant PC and allows for hypothesis-driven cause-and-effect studies of mechanisms underlying treatment response and resistance. *Prostate 77: 654–671, 2017.*

KEY WORDS: **prostate cancer; patient-derived xenografts; response to castration; bone response**

INTRODUCTION

Metastatic prostate cancer (mPC) is a deadly disease that is responsible for approximately 27,000 deaths per year in the United States. As most localized PCs are cured by primary intervention, a subset will recur with distant spread, and other men present with de novo mPC, for which there is no curative treatment. Despite initial responses to androgen deprivation therapy (ADT), mPC eventually progresses to metastatic castration-resistant PC (mCRPC) with highly variable responses to second-line androgen receptor (AR) targeted therapeutics, chemotherapy, and other targeted agents [1–7]. To improve outcomes, more effective therapeutics must be identified and the inter-individual heterogeneity of tumor drivers and mechanisms of resistance to treatments need to be defined and exploited.

Preclinical cancer models have the potential to rapidly advance drug development efforts. However, in vitro models, including cell lines and organoid systems, have well-recognized limitations [8,9]. In vivo experiments using human tumor cell lines as xenografts are limited by strong selective pressures produced by prior in vitro adaptation to culture conditions, and in many cases correlate poorly with clinical outcome [10,11]. An alternative approach is developing patient-derived xenografts (PDXs) that are initially established and subsequently passaged in murine hosts. Many PDX models retain key features of patients' tumors such as histologic architecture, genomic signatures, tumor heterogeneity, and in some situations, an influential stromal microenvironment [12]. PDXs have also been shown to more faithfully reflect clinical responses to cancer therapeutics and consequently have the potential to accelerate drug development [13,14].

The ability to comprehensively interrogate genomes and gene expression has enabled the underlying genetic drivers of tumor behavior to be integrated with assessments of response and resistance to drugs and to develop biomarkers predictive of treatment outcome [15]. Notably, drug studies involving panels of PDX models have identified molecular characteristics of PDXs that are concordant with responses observed in clinical studies involving the same drug [13]. This work provided a foundation for efforts to generate preclinical data that accurately predicts which drugs and drug combinations should be assessed clinically. As there is substantial molecular heterogeneity in tumors, preclinical models can also serve to provide insights into which tumor subtypes in patients are most likely to respond to a particular therapeutic [16,17]; and consequently, inform clinical trial designs where a companion predictive biomarker may be informative.

To realize the full potential of PDX models, it is useful to evaluate therapeutics efficacy across a spectrum of PDXs that reflect the tumor diversity observed in the clinic. However, only a few PC PDX models have been developed. A recent study describing ~1,000 PDX models, representing a wide range of human cancers, included no PC PDXs [13]. Moreover, existing PDX repositories (e.g., Jackson Laboratories) contain very few (n = 4) PC PDX models, a number which hardly represent the molecular diversity of human PC.

Our objective was to address a major limitation in the development of effective therapeutics for advanced PC by generating PDX models representing the diverse genotypes and phenotypes found across the spectrum of advanced PC. Here we report the characterization of 21 PC PDXs, designated the LuCaP series. We demonstrate that the LuCaP PDX models exhibit histologies, genetic alterations, and phenotypes concordant with patient specimens, and also recapitulate the heterogeneous responses to standard therapies observed in patients. The LuCaP PC PDX series is a clinically relevant platform to investigate the biology of advanced PC, evaluate therapeutics, and identify biomarkers predictive of treatment responses.

MATERIALS AND METHODS

Acquisition of Prostate Cancer Patient Tissues and PDX Establishment

Patient samples and clinical data abstraction. Tissue collection for research was approved by the University of Washington Human Subjects Division IRB,

which approved all Informed Consents that were used for tissue acquisition (IRB #39053). Tumors were acquired from patients who signed informed consent. The vast majority of implanted tissues was from metastatic foci obtained at tissue acquisition necropsy (TAN) in a manner which limited warm ischemic time as much as possible (aiming for 4–8 hr after death) [16]. A few samples were obtained from surgical procedures. Pertinent clinical information was abstracted from the patients' charts, including age, PSA levels, treatments, and treatment responses.

PDX establishment. All animal procedures were approved by UW Institutional Animal Care and Use Committee and according to NIH guidelines. Harvested tumor tissues were evaluated by pathologists, viable tumor tissue was macro dissected to minimize content of stroma, fat, and necrotic tissue. The tumor pieces were then immediately placed in ~10 ml of Dulbecco's Phosphate Buffered Saline (DPBS) with 20 mg/ml of Gentamicin for 5 min, rinsed with DPBS and cut into ~20 mg pieces (about 3–4 mm per cubed side) for implantation. Tumor bits were implanted subcutaneously in 6–8 weeks old intact male athymic Nu/Nu (NU-*Foxn1nu)* or CB-17 SCID (CB17/Icr-*Prkdcscid*/IcrCrl) mice (Charles River Laboratory) [18–20]. Mice were monitored for up to 18 months post implantation for initial growth. Tumors that grew were passaged into new intact male mice. We set three passages as an indication of an established PDX line. Tumor samples were harvested from later passages (>3) and frozen or embedded in paraffin for characterization. LuCaP PDXs are maintained by constant passaging in SCID mice.

LuCaP PDXs Molecular Characterizations

Histopathology and immunohistochemistry (IHC). Subcutaneous LuCaP PDX tumors were formalin fixed and paraffin embedded. Five-micrometer sections were cut and stained with hematoxylin and eosin (H&E) and results were compared with the originating tissues (as available). One-millimeter tissue cores from two different tumors of each PDX (33 lines) were punched in duplicates and embedded into tissue microarrays (TMA). TMA tissue sections were used for IHC analyses, which was standardized: primary antibodies at 4°C overnight (Table S1), followed by appropriate biotinylated secondary antibody (1:150), ABC reagent (Vector Laboratories), and DAB (Invitrogen). Mouse or rabbit normal IgG were used as negative controls, respectively. Immunoreactivity was typically assessed using a compositional scoring system—the multiplicand of each intensity level ("0" for no reaction product, "1" for faint and fine brown chromogen, and "2" for clear and coarse granular chromogen) by percentage of cells at each intensity. The final score was the sum of multiplicands. The distribution of final scores was grouped as "negligible" (score range: <3), "weak" (score range: 3–99), "moderate" (score range: 100–149), and "intense" (score range: 150–200) [21].

Single tandem repeat (STR) signatures. The STR signature was used to determine the unique identity of individual PDX line and to assure the identity and maintenance of the PDX lines (General Genetics Corporation). The STR analyses are repeated about every fifth to tenth passage, depending on growth rate of the PDXs.

RNA isolation and qRT-PCR. RNA isolated from subcutaneous tumors was used for qPCR analysis to evaluate expression levels of AR and ARV7, and RPL13a using Applied Biosystems 7,900 sequence detector as described previously [22] (Table S2). Two to three samples per PDX were used and reactions were run in triplicates. Expression levels were normalized to RPL13a.

Genomic analysis of DNA copy number. Genomic DNA was extracted from subcutaneous tumors using DNeasy Blood & Tissue Kit (Qiagen) and labeled with the Agilent Genomic DNA Enzymatic Labeling Kit (Cy3-dUTP). A pool of reference normal DNA (Promega) was labeled with Cy5-dUTP. Cy3 and Cy5 probes were combined and hybridized to Agilent 2×400 K SurePrint G3 CGH Microarrays following the manufacturer's specifications [23].

Genome-wide gene expression analyses. To evaluate gene expression, total RNA was extracted from subcutaneous PDX tissues as described above and Agilent array analysis was done as described previously using one tumor per PDX [24].

AR sequencing. Genomic DNA was extracted from subcutaneous PDXs and PCR amplified. AR primer sequences are listed in Table S2. Sanger Sequencing was performed using BigDye Terminator v3.1 Cycle Sequencing Kit (Life Technologies). Sequences were aligned to human AR genomic sequence NC_000023.11 and mRNA RefSeq NM_000044 using Sequencher Software (version 5.1, Gene Codes, Ann Arbor, MI). Mutations were verified using The Androgen Receptor Gene Mutations Database (McGill University).

Intra-tumoral Testosterone (T) and Dihydrotestosterone (DHT) measurements. Subcutaneous PDX tumors (30–100 mg) were used for T and DHT analyses using described LC-MS methodology [25]. Two or three tumors were used per PDX.

LuCaP PDX In Vivo Characterization

Responses to castration and docetaxel. Eighty intact male mice (CB-17 SCID, Charles River Laboratory) were implanted subcutaneously with tumor bits. When tumors exceeded ~100 mm^3 animals were enrolled in groups: group 1: intact male mice; group 2: castration; group 3: low dose docetaxel (5 mg/kg or 10 mg/kg docetaxel via intraperitoneal injection (IP) every other week (EOW)); and group 4: high dose of docetaxel (20 mg/kg docetaxel via IP once a week (QW)). To characterize docetaxel responses of the castration-resistant (CR) PDXs, tumor bits were implanted into castrated male SCID mice; group 1: castrated control; and group 2: high dose docetaxel (20 mg/kg docetaxel via IP QW). Tumor volume (TV) and body weight (BW) were measured once a week. Blood was collected every other week for determination of serum PSA levels (Total PSA Assay, Architect, Abbott Laboratories). Animals were sacrificed when tumors exceeded 1,000 mm^3 or if animals became compromised.

Establishment of CR PDX sublines. A sample of a tumor that regrew after castration (one tumor per line from group two above for each line) was harvested and immediately transplanted into castrated male SCID mice. These PDX lines are passaged in castrated male mice and designated with "CR" after the name of the parental lines and passaged in castrated hosts.

Bone response. Subcutaneous LuCaP PDX tumors were dissociated to a single-cell suspension and injected into tibiae of intact male SCID Beige mice (CB17.Cg-*Prkdc*^{scid}*Lyst*$^{bg\text{-}J}$/Crl, 4–6 weeks of age, Charles River Laboratories) as described previously [26]. Intra-tibial tumor growth was monitored by serum PSA levels where appropriate and by radiographs (MX-20, Faxitron X-ray Co.). Animals were followed for up to 5 months. Tumored tibiae were harvested at sacrifice, decalcified by EDTA (10% for 1–2 weeks) and embedded in paraffin for Goldner staining to evaluate bone response, as described [27].

Statistical Analyses

Statistical comparisons were made with GraphPad Prism software. All *P* values are two-sided. *P* values less than 0.05 were considered significant. Association of gene transcript with genomic copy number was tested by pairwise *t*-test to WT group using the pairwise *t*-test function in R.

RESULTS

General Characteristics of the LuCaP PDXs

Establishment of the LuCaP PC PDX series. During the period of 1991–2005, we collected 261 PC samples from 156 patients and implanted them subcutaneously into immunodeficient male mice. Of these, 26 were successfully propagated beyond three passages for an overall take rate of ~10% (Table I). Five of the PC PDX lines did not survive past passage five and were not further characterized. Ten of the stable PC PDXs were established from primary PC or PC metastases obtained from the operating room (OR). Eleven were established from mCRPC samples obtained through a tissue acquisition necropsy. In our series, we did not observe any consistent differences in the establishment rates of lines from metastases compared to primary tumors or from tumors acquired from the OR versus those obtain at TAN. We also did not observe any association of take rates with a specific metastatic site or time from death to implantation, though the low rate of establishing PC PDXs precludes a systematic analysis. Collectively, the 21 PC PDX models, designated the LuCaP PC PDX series, represent a spectrum of metastatic sites, histologies, and prior exposures to a variety of therapeutics used in the treatment of men with advanced PC (Tables II and III).

TABLE I. Prostatic Tissues Xenografting

Tissue type	Tissues implanted	Established PDXs
Primary PCa	21	4
Adrenal metastasis	2	0
Ascites	2	1
Bladder metastasis	7	1
Bone metastasis	54	2
Bowel metastasis	2	1
Lymph node metastasis	121	8
Liver metastasis	52	4
	261	21

2-5 mice per tissue.
Number of patients, 156; number of tissues, 261; long-term PDXs, 21.

TABLE II. LuCaP PDXs Characteristics

LuCaP	Date of transplant	Tissue implanted	Histology	Current passage	Time to 600–800 mg	PSA in serum	AR N-terminal (IHC)	ERG (IHC)	PTEN (IHC)	SYP (IHC)	Growth in bone	Response to castration	Response to docetaxel
LuCaP 23.1	1991	LN metastasis	AC	107	2.5–3.0	+++	+++	++	+	+	Yes/B	+++	+++[a]
LuCaP 23.1CR[c]	2013	EXP	AC	8[c]	2.5–5.0[c]	++[c]	+++	++	+	+	Yes/B	−	+++[a]
LuCaP 23.12	1991	LN metastasis	AC	NA	NA	+++	+++	++	+	+	ND	+++	+++
LuCaP 35	1993	LN metastasis	AC	150	2.0–2.5	+	++	+	−	−	Yes/M	+++	+++*
LuCaP 35CR	2001	EXP	AC	76	2.0–2.5	+	++	+	−	−	Yes/M	−	+++
LuCaP 49	1995	Omental fat metastasis	NE	113	3.0–3.5	−	−	−	−	++	Yes/M	−	++
LuCaP 58[b]	1996	LN metastasis	AC	103	2.5–3.0	+	+++	−	+	−	Yes/B	+	+++
LuCaP 70	1997	Liver metastasis	AC	93	3.0–3.5	++	+++	−	+	−	Yes/L	++	+++
LuCaP 70CR	2011	EXP	AC	17	3.5–4.0	+	+++	−	+	−	Yes/B	−	+
LuCaP 73	1997	Primary PCa	AC	101	2.5–3.0	++	+++	−	+	−	Yes/M	+++	+++
LuCaP 73CR	2011	EXP	AC	10	4.5–5.0	+	+++	−	+	−	ND	−	+/−
LuCaP 77	1998	Femur metastasis	AC	70	2.5–3.0	+++	+++	−	+	-	Yes/B	++	+++
LuCaP 77CR	2010	EXP	AC	25	3.0–3.5	++	+++	−	+	+++	Yes/B	−	+++
LuCaP 78	1998	LN metastasis	AC	41	4.5–5.0	++	+++	−	+	−	No	+++	+/−
LuCaP 78CR	2011	EXP	AC	8	5.5–6.0	++	++	−	+	−	ND	ND	ND
LuCaP 81	1998	LN metastasis	AC	31	5.5–6.0	+	+++	−	+	−	Yes/M	+++	+++*
LuCaP 81CR	2009	EXP	AC	10	5.5–6.0	+	+++	−	+	−	ND	ND	ND
LuCaP 86.2	1999	Bladder metastasis	AC	57	3.0–3.5	+++	+++	++	−	+	Yes/L	−	+++
LuCaP 86.2CR	2010	EXP	AC	21	3.0–3.5	++	++	++	−	+++	No	−	++
LuCaP 92	1999	LN metastasis	AC	104	4.0–5.0	++	++	+++	++	−	No	+++	+++
LuCaP 93	1999	TURP	NE	73	2.5–3.0	−	−	−	−	+++	Yes/B	−	++
LuCaP 96	1999	TURP	AC	62	2.5–3.0	+++	+++	−	−	−	Yes/B	+++	++[a]
LuCaP 96CR	2004	EXP	AC	41	5.0–5.5	++	+++	−	−	−	No	−	+++
LuCaP 105	2000	Rib metastasis	AC	54	3.0–3.5	++	+++	−	−	−	Yes/M	++	+/−
LuCaP 105CR	2010	EXP	AC	16	3.5–4.0	++	+++	−	−	−	ND	−	−
LuCaP 115	2001	LN metastasis	AC	NA	NA	+	++	−	+	−	ND	ND	ND
LuCaP 136	2004	Cells from ascites	AC	59	1.5–2.0	+/−	+++	−	−	−	Yes/B	+++	+
LuCaP 136CR	2012	EXP	AC	10	3.0–3.5	+/−	+++	−	−	−	ND	ND	ND
LuCaP 141	2005	TURP	AC	60	2.5–3.0	++	+++	−	+	−	Yes/L	+++	+++
LuCaP 145.1	2005	Liver metastasis	NE	31	3.0–3.5	−	−	−	+	+++	Yes/M	−	+++
LuCaP 145.2	2005	LN metastasis	NE	48	2.5–3.0	−	−	−	−	+++	Yes/M	−	+++[a]
LuCaP 147[b]	2005	Liver metastasis	AC	66	2.5–3.0	+/−	+++	−	−	−	Yes/M	+	+[a]
LuCaP 147CR[b]	2010	EXP	AC	23	2.5–3.0	+/−	+++	−	+	−	ND	−	−[a]

PSA: +++, >500; ++, 99–500; +, 5–100; +/−, 0.1–4.9; IHC, +++; IHC score 150-200; ++ 100–149; +: 3–99; −: <3; LN, lymph node; AC, adenocarcinoma; EXP, experiemtnally derived; TURP, trauurethral resection of prostate; NEPC, neuroendocrine prostate cancer; CR, castration-resistant B, blastic; L, lytic; M, mixed.

[a]Treatment increased body weight loss.

[b]Ulcerate readily response to castration: +++, TV decreases significantly for a prolong period of time; ++, tumors progress but slower than control tumors; +, negligible response; −, no response.

[c]Original LuCaP 23.1 CR was lost and a new line was generated.

TABLE III. PDXs and Patient's Clinical Information

LuCaP#	Date of transplant	Source	Tissue implanted	Age at diagnosis	Gleason score of primary	Time with disease prior tissue harvest (Yr)	Androgen ablation	CRPC disease	Chemotherapy and/or bisphosphonates
LuCaP 23.1	1991	TAN	LN metastasis	NA	NA	NA	NA	NA	NA
LuCaP 23.12	1991	TAN	Liver metastasis	NA	NA	NA	NA	NA	NA
LuCaP 35	1993	OR	LN metastasis	65	5 + 5	1.0	Y	Y	DES
LuCaP 49	1995	OR	Omental fat metastasis	67	3 + 5	4.8	Y	N	None
LuCaP 58	1996	OR	LN metastasis	61	4 + 5	0.2	N	N	None
LuCaP 70	1997	TAN	Liver metastasis	59	3 + 4	5.0	Y	Y	Corticosteroids; DES
LuCaP 73	1997	OR	RRP	47	4 + 5	1.9	Y	Y	Ketoconazole; Corticosteroids; DES
LuCaP 77	1998	TAN	Femur metastasis	65	NA	15.4	Y	Y	Mitoxantrone; DES
LuCaP 78	1998	TAN	LN metastasis	52	7	6.5	Y	Y	Taxol; Taxotere; Ketoconazaole; Corticosteroids; Mitoxantrone; DES
LuCaP 81	1998	TAN	LN metastasis	70	NA	4.6	Y	Y	None
LuCaP 86.2	1999	OR	Bladder metastasis	65	NA	14.1	Y	Y	None
LuCaP 92	1999	TAN	LN metastasis	56	9	1.4	Y	Y	Ketoconazole; Corticosteroids
LuCaP 93	1999	OR	TURP	84	7	1.5	Y	N	None
LuCaP 96	1999	OR	TURP	61	5 + 4	0.5	Y	N	None
LuCaP 105	2000	TAN	Rib metastasis	48	5 + 3	5.1	Y	Y	Taxol; Taxotere; Ketoconazole; Mitoxantrone; Bisphosphonates
LuCaP 115	2001	OR	LN metastasis	59	3 + 3	10.8	Y	Y	Ketoconazole
LuCaP 136	2004	OR	Cells from ascites	62	5 + 5	0.6	Y	Y	None
LuCaP 141	2005	OR	TURP	73	NA	6.3	Y	Y	Taxotere; Ketoconazole; Corticosteroids; Bisphosphonates
LuCaP 145.1	2005	TAN	Liver metastasis	59	4 + 5	2.4	Y	Y	Ketoconazole; Corticosteroids; Bisphosphonates
LuCaP 145.2	2005	TAN	LN metastasis	59	4 + 5	2.4	Y	Y	Ketoconazole; Corticosteroids; Bisphosphonates
LuCaP 147	2005	TAN	Liver metastasis	67	4 + 5	2.2	Y	Y	Taxotere; Ketoconazole; Corticosteroids; DES; Bisphosphonates

TAN, tissue acquisition necropsy; OR, operating room; TURP, transurethral resection of prostate; LN, lymph node; RRP, radical prostatectomy; NA, not available.

Growth characteristics of LuCaP PDXs. Establishment of PC PDXs is known to be difficult with a low take rate and long time to initial growth. In our series we achieved approximately 10% establishment rate of stable PC PDXs with the time to initial growth from four up to over 12 months. After the initial growth, the LuCaP PDXs are passaged in mice. The established LuCaP PDXs have differential growth characteristics: take rates of secondary passages ranges from 50% to 80%; with the exception of LuCaP 92, which has a very low take rate (10–30%). The time from implantation to initial growth of secondary passages ($\sim$50 mg) ranges from 6 to 36 weeks. The time from the initial growth to $\sim$1,000 mg ranges from 4 to 16 weeks. It is important to note that the LuCaP PDXs are biologically heterogeneous; the PDXs vary in take rates and time to initial growth between the sequential passages, and even exhibit variability in growth characteristics of PDXs grown from the same tumor donor.

Establishment of castration-resistant PDXs. While a majority of the PC patients from which the LuCaP PDX lines were derived received ADT and progressed to CRPC, several of the PDXs implanted in intact male mice responded to castration with tumor regression. This response may be attributed to the lower androgenic conditions in castrate mice compared to humans [28]. Tumors that regrew after castration were harvested and re-implanted into castrated male mice to establish castration-resistant (CR) sublines. Twelve CR PDXs were established and are continually propagated in castrated hosts (Table II).

Fidelity of PDXs to the source tumor. PC is a heterogeneous disease with multiple morphological patterns, and the LuCaP PDXs exhibit diverse histological features that recapitulate the histologies observed in the patients' source tumors. For example, LuCaP 86.2 and LuCaP 96 are well-differentiated adenocarcinomas, LuCaP 147 is a poorly differentiated adenocarcinoma, and LuCaP 145.1 is a neuroendocrine carcinoma, as are the respective originating tumors. Immunohistochemical profiles are also generally maintained in the LuCaP PDXs (Fig. 1). Rarely did we observe significant alteration of protein expression during passaging of LuCaP PDXs. One such example is ERG expression in later passages of LuCaP 86.2, while the first four passages and the originating metastasis were ERG negative. However, the vast majority of protein expression levels were concordant and relatively stable across multiple passages of each line.

STR profile. To ensure the originality and maintenance of genotype of each line we perform STR analyses of the PDXs and each line has a specific STR profile (Table S3) that is checked every 5–10 passages. CR lines show the same STR profile as the parenting androgen-sensitive lines (data not shown).

Molecular Characteristics of the LuCaP PDXs

Genomic alterations. Multiple recurrent chromosomal alterations occur in mCRPC [16,29,30]. We assessed genomic alterations in the LuCaP PDXs by array comparative genomic hybridization (CGH). The chromosomal alterations in LuCaP PDXs are concordant with those commonly found in CRPC patient metastases (Fig. 2A and B). Recurrent events include *AR* amplification (8/21; 38%), *PTEN* loss (8/21 heterozygous loss; 4/21 homozygous loss; overall 57%), *RB1* loss (10/21 heterozygous loss; 6/21 homozygous loss; overall 76%), and TMPRSS2-ERG rearrangement (10/21; 48%). In the experimentally derived CR sublines, the genomic aberrations are generally concordant with the original PDX with a few exceptions including *AR* amplification following castration in five lines (Fig. 2B). Furthermore, our characterization data also show that three models have a hypermutated phenotype with microsatellite instability and mismatch repair enzyme mutations [31]. In some instances, we were able to establish multiple PDXs from the same patient but from different metastases. LuCaP 23.1 originated from a lymph node metastasis and LuCaP 23.12 from a different lymph node metastasis of the same patient. Similarly LuCaP 145.1 originated from a liver metastasis and LuCaP 145.2 from a lymph node metastasis of the same patient. These two sets of PDX models demonstrated numerous concordant genomic aberrations but also a degree of diversity (Fig. 2B). Differential characteristics of the PDXs from the same patient demonstrate the heterogeneity of PC metastases within a single patient.

AR expression and activity. AR is a key transcription factor in PC biology and progression. Seventeen of the original 21 LuCaP PDXs are adenocarcinomas that express AR and exhibit AR-transcriptional activity based on the expression of AR-regulated genes and proteins including PSA. Four of the LuCaP PDXs are NE PC which express synaptophysin, but lack AR and PSA (Fig. 2C).

AR mutations. Mutations in the AR ligand binding domain occur frequently in mCRPC and contribute to disease progression and treatment resistance. Eight of the 33 LuCaP PDXs (4/21 original and 4/12 CR lines) exhibit *AR* mutations (Table IV) LuCaP 73 and LuCaP 73CR PDX models have the well-characterized AR gain of function mutation, V715M, which promotes

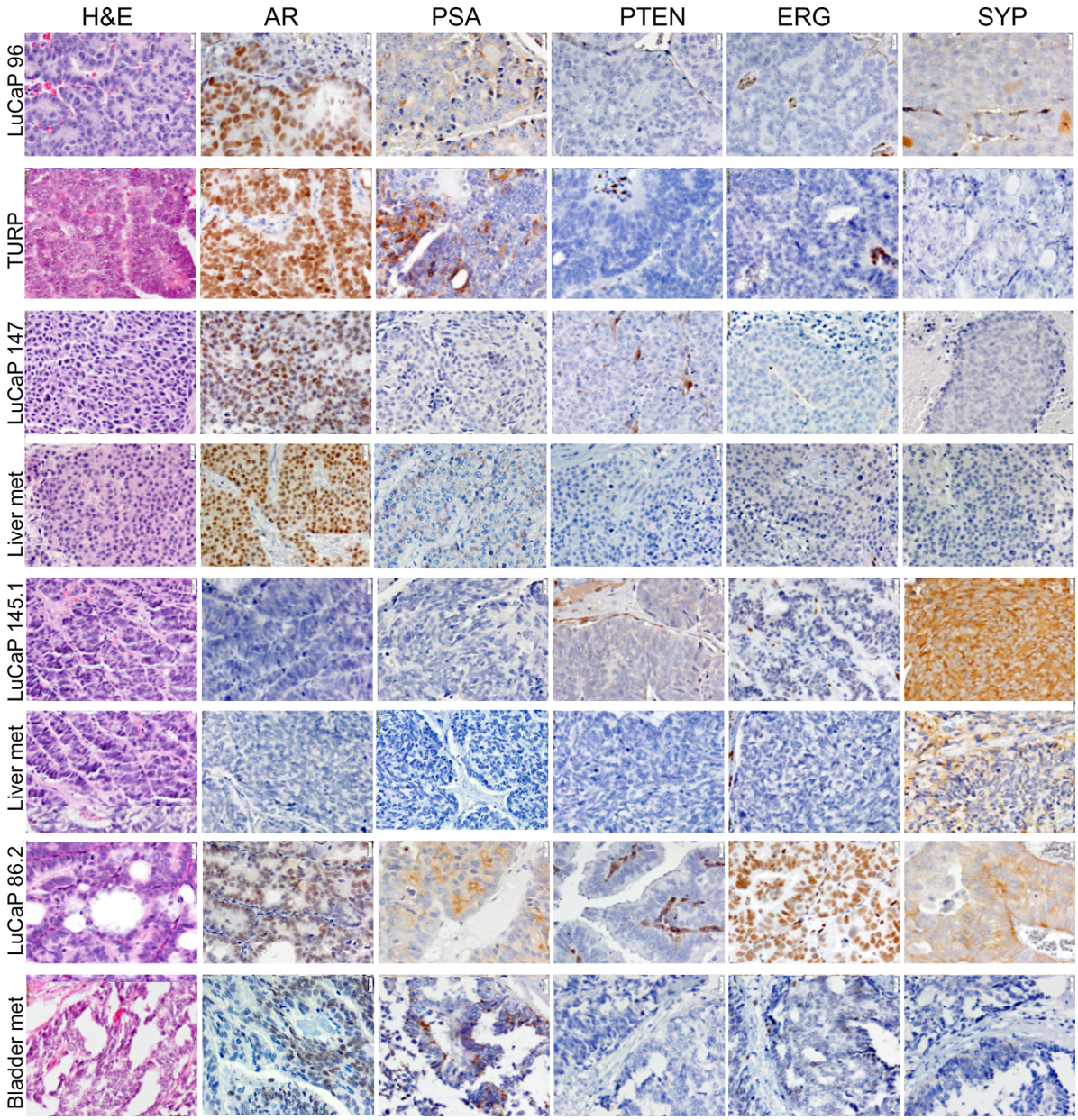

Fig. 1. LuCaP PDXs and the originating tissues H&E and IHC of four representative LuCaP PDXs and their originating metastases are shown. Paraffin embedded metastases and subcutaneous PDX tumors were used. The PDXs maintain morphology of the originating metastases. AR, PSA, PTEN, ERG, and SYP expression (as representative markers) in the LuCaP PDXs also show, in general, concordance with the originating tissue, with an exception of LuCaP 86.2 that expresses ERG and SYP while the originating metastasis was negative.

AR activation by estrogen and progesterone. LuCaP 147 and LuCaP 147CR harbor the H874Y AR mutation, which was originally reported in the CRW22 xenograft model and can be activated by cortisol, estradiol, DHEA, and hydroxyflutamide. The LNCaP AR mutation T877A was detected in LuCaP 73, LuCaP 73CR, LuCaP 78, and LuCaP 78CR and in LuCaP 147CR. These mutations in the ligand-binding domain also promote AR activation at low concentrations of T, and DHEA [32,33].

AR transcript quantification. AR mRNA amounts vary substantially across the adenocarcinoma LuCaP PDXs (Fig. 3B). While the neuroendocrine PDXs do not express AR transcripts (Fig. 3B). Our results also demonstrate upregulation of AR mRNA in CR PDX, with 2–11 fold increases in matched CR PDXs and their original androgen-dependent (AD) lines. LuCaP 86.2 PDX is a notable exception—with no increase in AR mRNA in the CR subline. This might be due to expression of ARV^{567}, negating

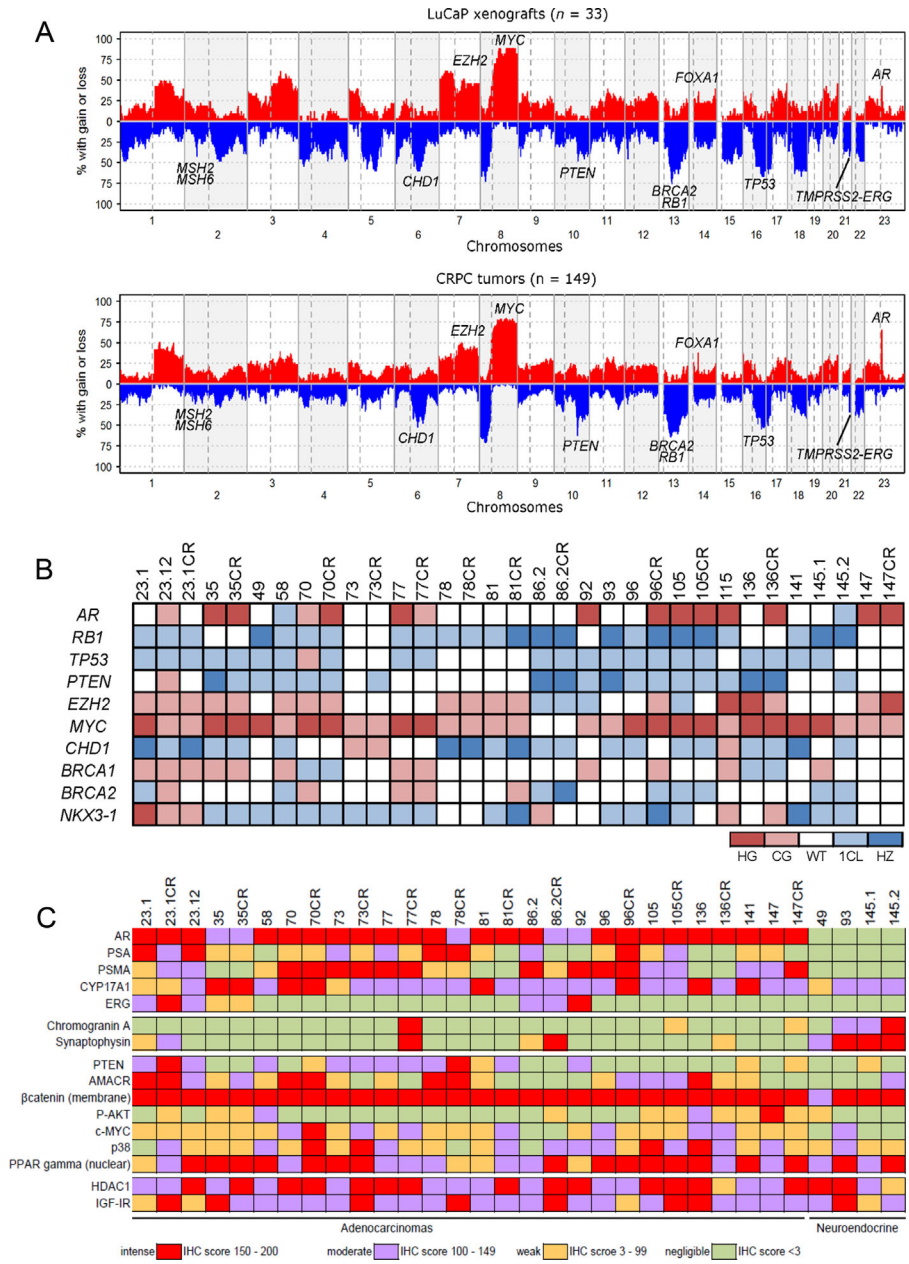

Fig. 2. Genomic and IHC analyses of LuCaP PDXs. (**A**) Frequency of copy number alterations in LuCaP PDXs (n = 33: 21 LuCaP PDXs and 12 experimentally derived castration-resistant LuCaP PDXs, top panel) and CRPC metastases (n = 149 from 60 patients; bottom panel (16)). Segmented data are sorted by chromosomal position; vertical-dotted lines indicate centromere position of each chromosome; y-axis, percentage of tumors with gains (segment threshold >0.3) in red or losses (segment threshold <−0.3) in blue. Selected genes of interest in peak regions of gain or loss are shown. (**B**) Alteration of copy number of selected genes in LuCaP PDXs; (**C**) IHC analysis of LuCaP PDXs. IHC Score is plotted. Adenocarcinomas express AR and AR-regulated proteins while neuroendocrine PDXs express chromogranin A and/or synaptophysin. HG, high gain; CG, one copy gain; WT, wild type; 1CL, heterozygous loss; HZ, homozygous deletion.

the requirement for increased wild type AR to maintain the AR transcriptional activity at low androgen levels [34].

AR transcript splice variants. One of the mechanisms of resistance to primary and secondary ADT is increased expression of spliced variants of AR that are constitutively active. To date, multiple AR transcript splice variants (ARVs) have been reported, most with loss of the ligand-binding domain. Clinical data indicate that several ARVs, most prominently, ARV7, are associated with resistance to primary and

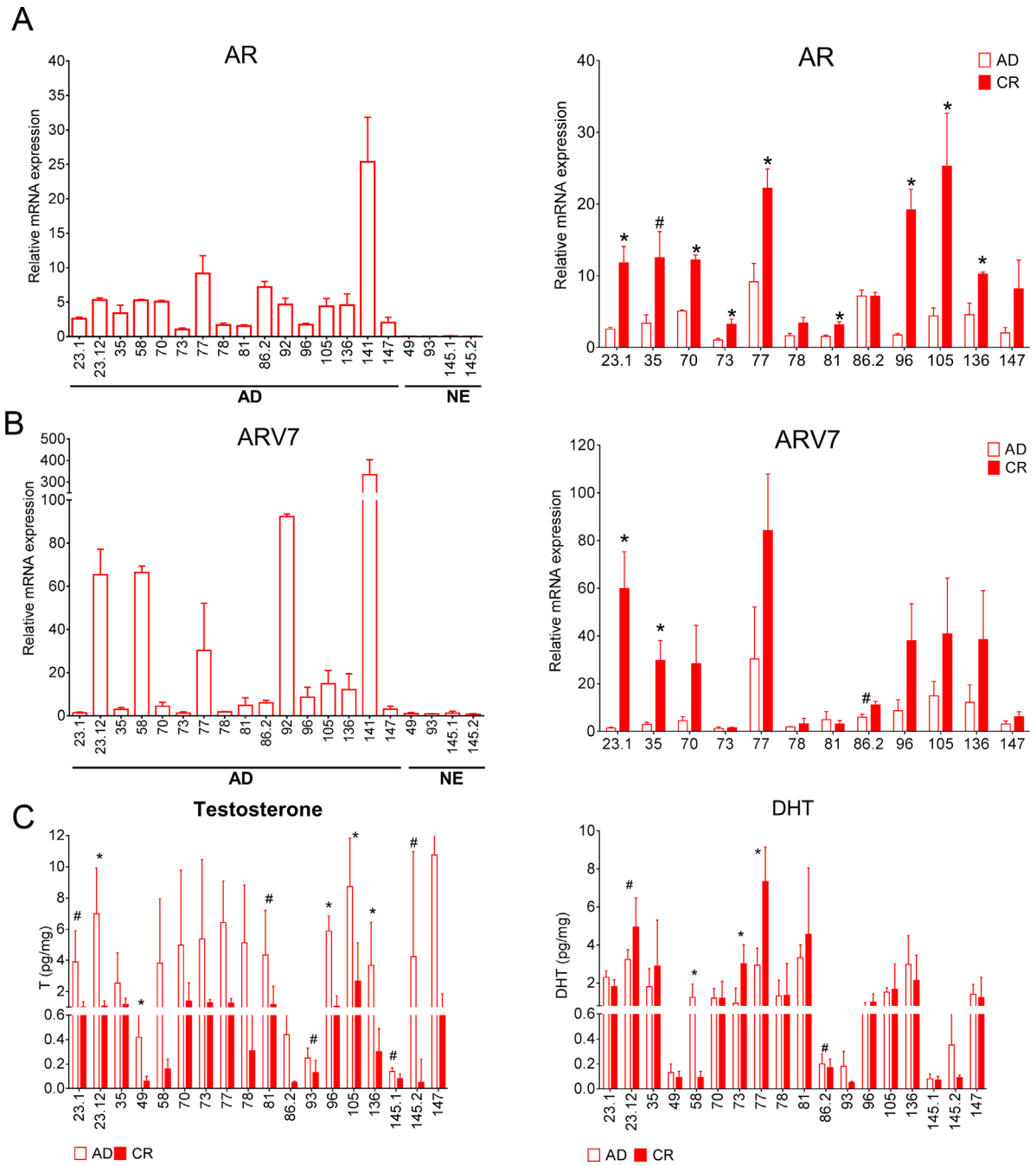

Fig. 3. AR expression, and intra-tumoral androgens. (**A** and **B**) AR and ARV7 Expression. RNA was isolated from subcutaneous tumors (n = 2–3 per model). AR and ARV7 mRNA levels were normalized to RPL13a and expressed relative to the LuCaP 73 value using ΔΔCT method. LuCaP 73 value was arbitrarily assigned an abundance value of 1. (**C**) T and DHT levels were determined in tumors using LC-MS (n = 2-3 per PDX). The mean ± SEM are plotted. $^{*}P < 0.01$; $^{\#}P < 0.05$. LB, ligand binding domain; NT, N-terminus; AD, androgen dependent; NE, neuroendocrine.

secondary ADT [35,36]. When comparing ARV7 expression in the adenocarcinoma PDXs we found a 200-fold difference in ARV7 transcript levels with lowest ARV7 in LuCaP 73, and high levels in LuCaP 141. Our analyses also clearly show the increased expression of ARV7 in CR disease; all CR sublines of the LuCaP PDXs except one (LuCaP 81CR) had higher levels of ARV7 ranging from 1.2- to 43-fold increase in paired CR sublines (Fig. 3C). In addition to ARV7, we have also shown that LuCaP 86.2 expresses ARV^{567} another constitutively active AR variant [34].

TABLE IV. AR Mutations in LuCaP PDXs

LuCaP xenograft	Type of mutation	Domain	Exon	Base pair change	Codon change
73, 73CR	Gain of function	LB	4	3261G>A	V715M
147, 147CR	Gain of function, deletion	LB, 3′ UTR	8, 3′ UTR	3738C>T, del T 4037	H874Y
73, 73CR, 78, 78CR, 147CR	Gain of function	LB	8	3747A>G	T877A
23.1, 23.1CR, 78, 78CR	Silent	NT	1	1754G>A	E212E

Genomic DNA was used to evaluate AR mutation status (n = 1 per PDX). LB, ligand binding domain; NT, N-terminus; AD, androgen dependent; NE: neuroendocrine.

Intra-tumoral androgens. The extragonadal synthesis of androgens within PC cells, either de novo or using adrenal androgen precursors promotes survival and growth of PC following ADT [37]. We measured intratumoral T and DHT in several parental LuCaP PDX lines grown in intact male mice and in tumors that regrew after castration. Intra-tumoral levels of T ranged from 0.14 to 11 pg/mg in tumors prior to castration and dropped after castration in all models (range 35–90% decrease). Intra-tumoral levels of DHT ranged from 0.1–3 pg/mg in PDX tumors from intact mice. However, in contrast to T, concentrations of DHT increased in several of the PDXs that regrew after castration while decreasing in others (Table IV). Our data also show that T and DHT levels are substantially lower in the NE PDXs and LuCaP 86.2 than in the other adenocarcinoma PDXs, suggesting either that the intra-tumoral synthesis is not active in the PDXs that are not responsive to ADT or, alternatively, that androgens are not retained in the tumors that do not express AR or express mainly AR variant that lacks ligand binding domain.

Molecular fidelity during long-term passaging. Early passages of PDX lines are thought to be the most similar to the originating tumors and are considered the best models of the human disease. However, it has been challenging to re-establish the growth of LuCaP PDXs after cryopreservation, nor do these models grow readily in vitro. Therefore, the LuCaP PDXs are maintained by continuous growth in mice. The current passages of the LuCaP PDXs are in a relatively high range (10–150 passages; Table II). Therefore, we assessed the effects of long-term passaging on the models. Genome-wide gene expression analyses showed clustering of the early and late passages of each individual LuCaP PDX, indicating maintenance of the general phenotypes of each PDX during prolonged growth in mice (Fig. S1A). If the murine environment substantially influenced the PDX phenotype over time, one may expect to see clustering of early passages of the PDXs versus late passages. Though other investigators found a higher content of murine tissue-derived transcripts in later PDX passages [13], we did not observe a significant change.

Transcriptome and whole exome sequencing analyses. We assessed the gene expression program of each PDX by genome-wide microarray hybridization (GSE66187). We also evaluated concordance between the transcriptomic and genomic data for well described PC associated genes of interest. We observed significant associations between copy number alteration and gene transcript levels (Fig. S1B). We have previously reported the spectrum of DNA mutations in the LuCaP PDX series using whole exome sequencing [38] (http://trace.ncbi.nlm.nih.gov/Traces/sra/?study=SRP008162).

LuCaP PDX Responses to the Therapeutics

Responses to ADT. Since the first line of therapy for advanced and recurrent PC is ADT, we evaluated LuCaP PDX responses to castration. While most patients respond well to primary ADT, a subset exhibit only transient remissions or no response. Collectively, the LuCaP PDXs also exhibited variable outcomes following ADT from complete tumor regression to overt tumor progression (Fig. 4 and Table II). Notably, variable responses to castration were detected even between animals bearing the same PDX, most probably related to cellular heterogeneity and stroma content, (Fig. 4B). This is an important issue to address when designing preclinical studies with a single PDX in order to power the study appropriately accounting for variable responses. In the clinical setting serum PSA levels are used to evaluate patient responses to therapy. In the assessments of PDX responses to ADT, serum PSA closely followed changes in TV after castration; again with variability between and within PDX lines (Fig. 4C). Similar to clinical observations, the majority of tumors adapt to castrate conditions and eventually regrow as CR disease. Overall, ADT results in survival benefits of adenocarcinoma PDX models that ranged from

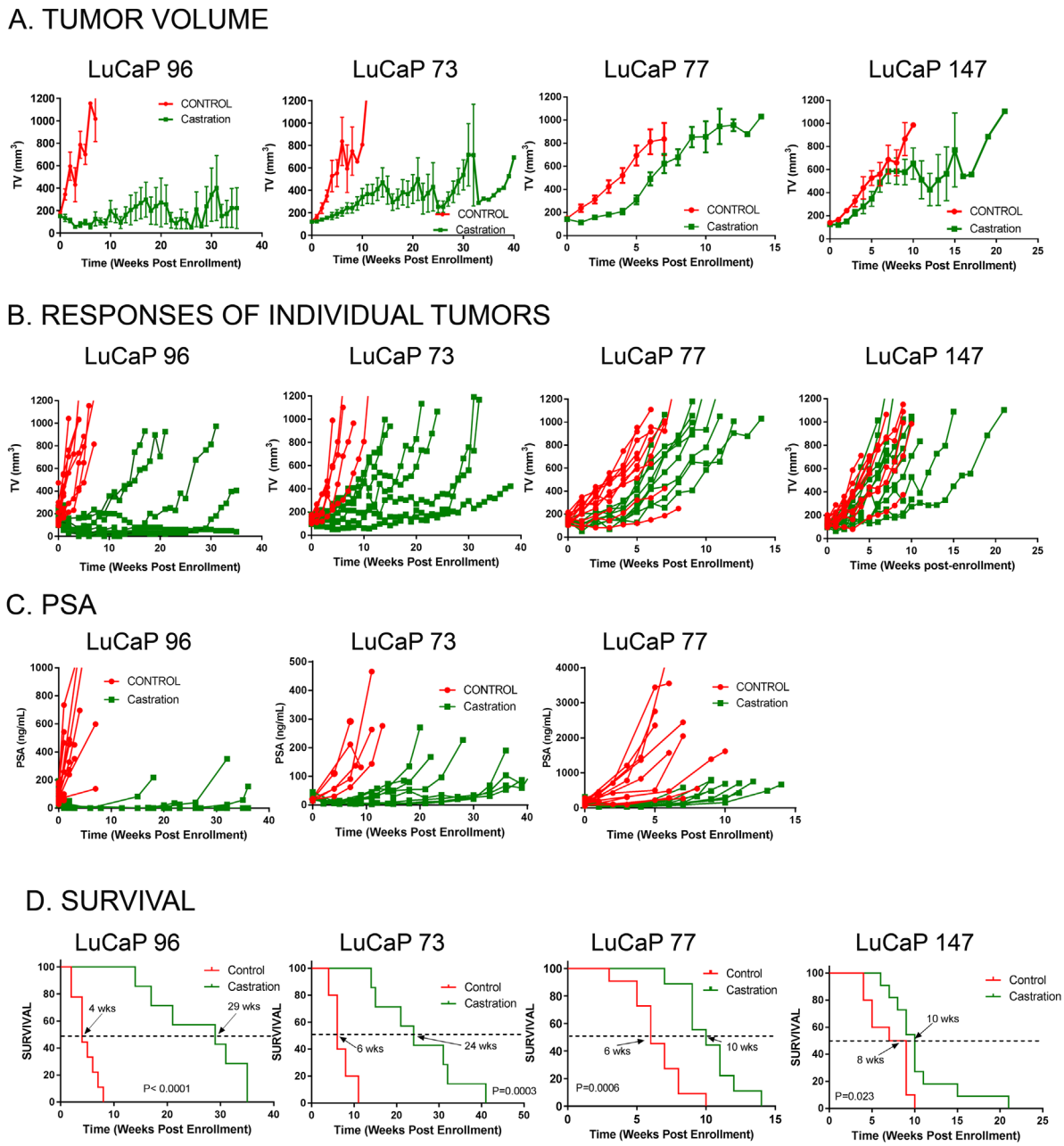

Fig. 4. LuCaP PDXs responses to castration. The LuCaP PDXs shown were selected to span the large scale of differential responses. Intact animals were implanted with tumor bits subcutaneously and when tumor exceeded 100 mm^3 animals were castrated and tumor volume response was monitored. (**A**) We observed prolonged to minimal response in attenuation of tumor progression; average TV $\pm$ SEM is plotted. (**B**) Responses of individual animals are plotted. (**C**) Decreases of serum PSA levels (animals bearing LuCaP 147 do not have measurable PSA in serum). It is important to note the variability of the responses of the same tumor in different animals. This is a result of heterogeneity of the PDXs. (**D**) Improvements in survival. The LuCaP PDXs shown were selected to span the large scale of differential responses.

increases of 25 weeks (LuCaP 96) to only 2 weeks (LuCaP 147), to no benefit in the NE LuCaP PDXs (LuCaP 49, LuCaP 93, LuCaP 145.1, and LuCaP 145.2) and LuCaP 86.2 (Fig. 4D and data not shown). Using the expression array results we queried association of AR expression and AR-activity with responses to castration. The CR PDXs tend to have higher levels of AR mRNA, which is concordant with increased *AR* copy number in these lines, but weaker AR-signaling activity when compared to the adenocarcinomas grown in intact male mice (Fig. S1C). There was no significant association of responses to castration with

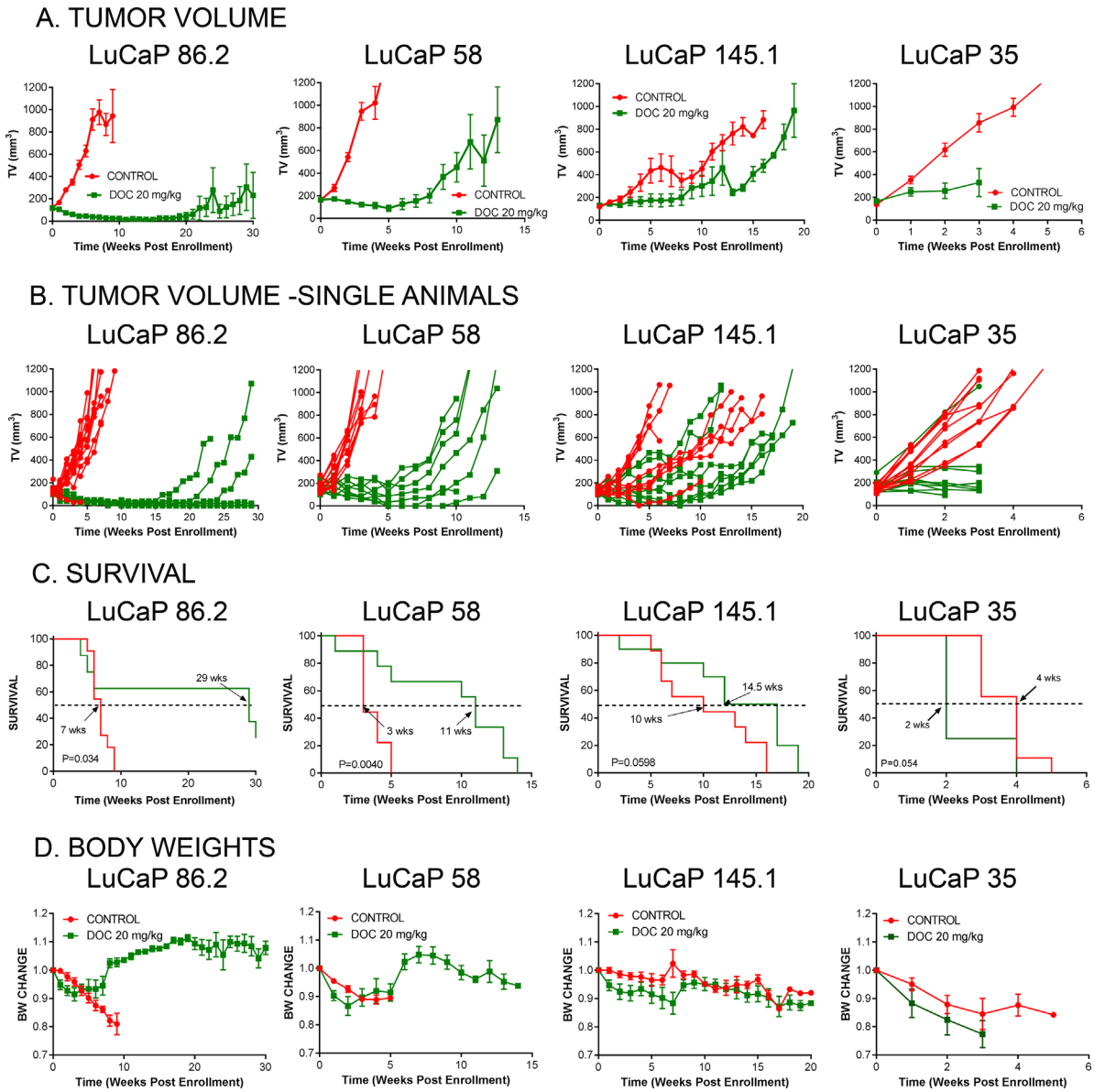

Fig. 5. LuCaP PDXs responses to docetaxel. The LuCaP PDXs shown were selected to span the large scale of differential responses. Intact animals were implanted with tumor bits subcutaneously and when tumor exceeded 100 mm^3 animals were treated with 20 mg/kg docetaxel by IP once a week, and tumor volume response was monitored. (**A**) We observed variable attenuation of tumor progression; mean ± SEM is plotted. (**B**) There was also variability of responses between animals bearing the same tumor. (**C**) Docetaxel treatment also resulted in improvement of survival with some models but not all. (**D**) Effects of the treatment on body weight. In the examples shown the treatment did not reduce body weight losses caused by tumor. Moreover, DOC treatment resulted in increased body weight loss of animals bearing some PDXs (e.g., LuCaP 35). Normalized body weight to beginning of the treatment is plotted (mean ± SEM).

AR expression or AR signaling activity. Trend toward a negative association was detected between intra-tumoral T levels and response to castration ($R = -0.68$, $P = 0.063$) indicating the involvement of intra-tumoral T synthesis in response to castration.

Responses to docetaxel. Docetaxel was the first chemotherapy shown to extend survival in men with mCRPC and remains in widespread use [7]. As with ADT, the duration of clinical responses to docetaxel vary substantially. We evaluated responses of LuCaP PDX lines to low dose and high dose docetaxel. In the majority of LuCaP PDX lines high dose docetaxel suppressed tumor growth and resulted in survival benefits though, as in patients, the improvement of survival varied widely. Of interest, docetaxel treatment reduced the survival of mice implanted with several PDX lines, notably LuCaP 35, because of

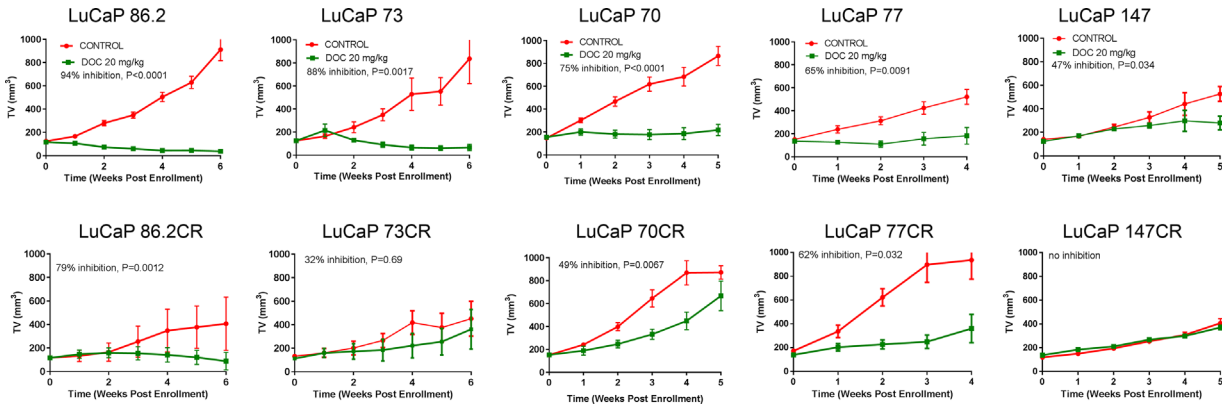

Fig. 6. Differential responses of androgen-dependent and castration-resistant PDXs to Docetaxel. Intact or castrated animals were implanted with tumor bits subcutaneously as appropriate and when tumor exceeded 100 mm^3 animals were treated with 20 mg/kg docetaxel by IP QW, and tumor volume responses were monitored for 6 weeks. The tumors that grew in intact animals (top panel) showed more pronounced tumor inhibition than their matched castration-resistant lines bottom panel). Average TV $\pm$ SEM is plotted.

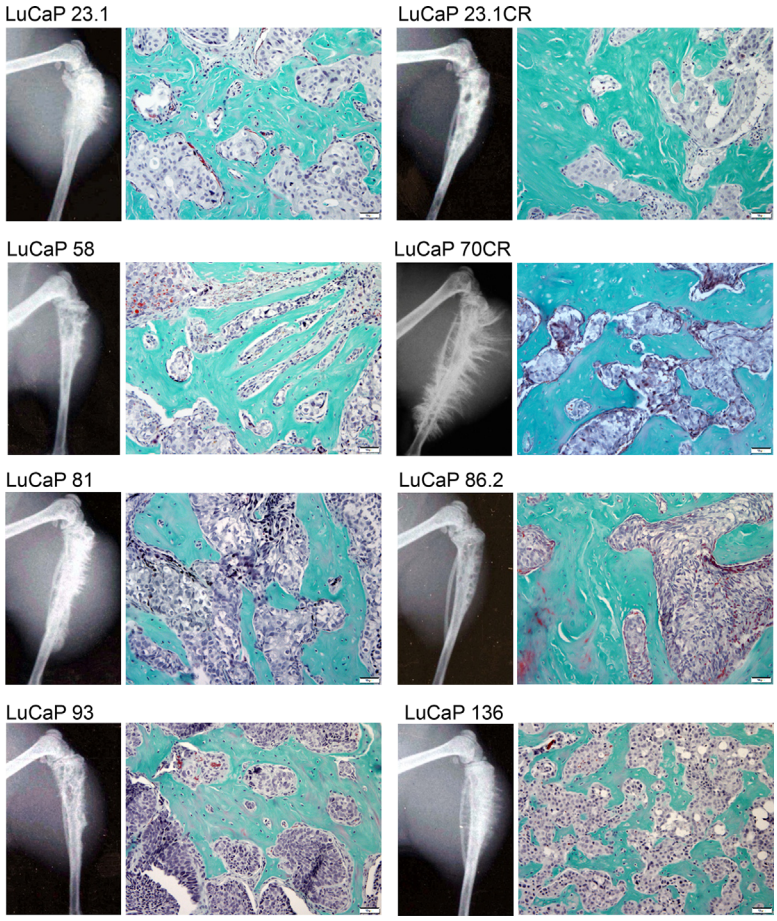

Fig. 7. Tumor bone interactions: osteoblastic reaction. Subcutaneous LuCaP PDXs were dissociated to a single cell suspension and injected into the tibiae of male mice. Tumor growth was monitored by serum PSA and/or radiography. Goldner's stain was used to visualize mineralized woven bone (light green), and tumor cells (purple). An osteoblastic reaction of the bone is demonstrated by a large volume of new woven bone and replacement of bone marrow with tumor cells.

significant decreases in body weight, despite the inhibition of tumor progression (Fig. 5 and Table II). Since the animals bearing these tumors were treated with the same dose and regimen as animals bearing other PDX tumors where survival improvements were observed, BW loss is not simply a negative side effect of docetaxel, but is a consequence of specific interactions between tumor, chemotherapy, and effects on the host. The low dose of docetaxel showed efficacy only in LuCaP 86.2 (data not shown), reflecting a rare exceptional responder to docetaxel [39].

Though docetaxel chemotherapy has been used primarily in mCRPC, the use of docetaxel earlier in treatment has been reported to produce survival benefits when given concurrently with initial ADT [40]. Based on the efficacy of docetaxel in PC before it develops castration-resistance, we compared docetaxel effects on the progression of androgen-sensitive and castration-resistant PDX pairs. We observed more pronounced inhibition of tumors growing in intact male mice versus their CR sublines (Fig. 6) supporting the potential benefits of a docetaxel treatment prior to the development of CRPC. Analyses of tissues from these studies may provide insights into the greater benefit of using docetaxel in androgen-sensitive tumors.

Characterization of bone responses to prostate cancer. The second most common site of PC dissemination is bone, and bone metastases are a source of significant morbidity. To effectively treat bone metastases, it is important to better understand interactions of PC cells and the bone microenvironment. Unfortunately most PC models, including the LuCaP PDXs, do not spontaneously metastasize to bone from subcutaneous tumors and even in the few cases where we evaluated tumor cell dissemination after orthotopic implantation we did not identify bone metastases [41]. To specifically assess tumor cell and bone microenvironment interactions, we directly injected tumor cells from LuCaP PDXs into murine tibia and followed tumor development and bone responses [26]. Of the 25 lines studied, 21 were able to proliferate to some extent in bone, but the take rates were highly variable ranging from 10% for LuCaP 145.2% to 80% for LuCaP 58. As in the clinical scenario, the bone responses were osteoblastic, mixed, and/or osteolytic (Table II). Importantly nine of the lines elicited a pronounced osteoblastic response (Fig. 7). Interestingly, the PDXs established from bone metastases did not show better take rates or growth in the bone versus the PDXs derived from soft tissue metastases. The most pronounced osteoblastic reaction was elicited by LuCaP 23.1, which originated from a lymph node metastasis. Detailed characteristics of the highly osteoblastic response to LuCaP 23.1 and the mixed/osteolytic/osteoblastic reaction to LuCaP 35 in bone was published previously [26].

DISCUSSION

PC is a heterogeneous disease with variation in gene expression, structural genomic aberrations, epigenetic states, predilection for metastatic spread, and responses to therapeutics. We have established a series of PC PDXs that reflect key molecular features and clinical phenotypes observed in human disease [31,38,42], including *AR* amplification, expression of AR splice variants, *PTEN* and *RB1* loss, *TP53* mutation, *TMPRSS2-ERG* rearrangements, hypermutation, NE differentiation, intra-tumoral T and DHT synthesis, and variable responses to ADT and docetaxel chemotherapy.

The paucity of PC PDX models clearly reflects the difficulties with xenografting prostatic tissues. To establish a PC PDX, the most critical step is access to tissues of good quality and viability. While primary PC is relatively easy to obtain in view of the frequency of prostate biopsy and radical prostatectomy procedures, metastases of CRPC are difficult to obtain, and, when acquired, are often of limited quantity. Our success in establishing mCRPC LuCaP PDXs is based on taking advantage of a robust tissue procurement program that acquires metastatic tissues through a TAN protocol [43,44]. The second critical step is the successful engraftment of tissues into suitable recipient animals. Several technical improvements to the xenografting protocol have improved PC take rates, including the use of murine hosts with more compromised immune systems, subrenal implantation, recombination of tissues with mesenchyme, and supplementation with T. Despite these advances, PC tissue is still challenging to establish as a PDX.

We and other investigators, and pharmaceutical companies have used the LuCaP PDX models to investigate fundamental features of PC biology and to evaluate therapeutic agents designed to treat PC. Results of these studies clearly indicate relevance of these models for identifying therapeutic targets and conducting early-phase research that support further clinical evaluations (Supplemental references). To date, the vast majority of our studies have evaluated a small number of PDX models, generally matching a particular tumor characteristic with a drug mechanism of action, rather than assessing responses across all available models. However, we have characterized all lines with respect to the two most commonly employed standard of care therapies for PC: ADT and docetaxel. We observed a wide-range of responses to

these modalities, as also occurs in men with PC. Notably, results of studies using LuCaP PDXs identified AR amplification/activity as an important mechanism of resistance to ADT [45], supporting the use of enzalutamide (now FDA-approved for men with mCRPC) [45,46], and also identified AR splice variants as an important mechanism of resistance to ADT [34,47] which supported the development of new AR N-terminal antagonists [48].

In the context of translational research, PDX models can be used in the drug development pipeline using a PDX Clinical Trials (PCT) approach. This strategy uses multiple PDXs with different characteristics, which reflects a traditional phase II clinical trial without pre-selection for a particular tumor characteristic. A major limitation hindering the more widespread adoption of PCT centers on the limited number of PDX models. This is particularly true for PC. This limitation severely curtails the opportunities afforded by PDX clinical trials in advancing novel drugs and drug combinations into the clinic, and particularly identifying an individual molecular vulnerability which could be exploited by enriching a trial population and developing a companion predictive biomarker. The existing LuCaP PDX series provides opportunities for conducting PC PCTs. To enhance such studies, we continue our efforts to generate additional mCRPC PDXs that (i) use tumors that were exposed to new FDA approved agents; (ii) exhibit both recurrent and rare molecular aberrations in AR-driven mCRPC; and (iii) include the new emerging phenotype/genotype of AR-null PC aggressive variant PC.

CONCLUSIONS

In this article, we present characterization data of multiple advanced prostate cancer PDXs, designated the LuCaP series, that maintain biological characteristics of the originating tumor including genomic and phenotypic features. Our in vivo results also show that the LuCaP series of PDXs recapitulate well the heterogeneous character of the advanced PC in patients and responses to standard-of-care treatments, that is, androgen deprivation and cytotoxic chemotherapy. Collectively, the LuCaP PDX series reflects the diverse molecular composition of human CRPC and allows for hypothesis-driven cause-and-effect studies of mechanisms underlying treatment response and resistance.

ACKNOWLEDGMENTS

We thank the patients and their families as well as their referring clinicians. We also thank multiple scientists who provided excellent technical assistance with this work throughout the years; including Kent Buhler, Janna Quinn, Jennifer Noteboom, Michiyo Dalos, Jessica Heide, Daniel Sondheim, Belinda Nghiem, Bryce Lakely, Ruth Dumpit, Roger Coleman, and Brett Marks.

AUTHORS' CONTRIBUTIONS

Conception and design: EC, RLV, PHL, PSN, TCH; development of methodology: EC, HMN, CM, LB, XZ, IC, LDT, RLV, EMM, MR, PSN; acquisition of data: EC, HMN, CM, LB, XZ, IC; analysis and interpretation of data: EC, HMN, CM, LB, LDT, XZ, RLV, IC, EMM, PSN, HML; writing, review, and/or revision of the manuscript: EC, HMN, CM, LB, TSH, IC, EMM, LDT, XH, HML, PSN, RLV, MR.

REFERENCES

1. Sweeney CJ. CECOG: CHAARTED—ChemoHormonal therapy versus androgen ablation randomized trial for extensive disease in prostate cancer. Clin Adv Hematol Oncol 2006;4: 588–590.
2. Attard G, Reid AH, Olmos D, de Bono JS. Antitumor activity with CYP17 blockade indicates that castration-resistant prostate cancer frequently remains hormone driven. Cancer Res 2009;69: 4937–4940.
3. Attard G, Reid AH, Auchus RJ, Hughes BA, Cassidy AM, Thompson E, Oommen NB, Folkerd E, Dowsett M, Arlt W, de Bono JS. Clinical and biochemical consequences of CYP17A1 inhibition with abiraterone given with and without exogenous glucocorticoids in castrate men with advanced prostate cancer. J Clin Endocrinol Metab 2012;97:507–516.
4. Scher HI, Fizazi K, Saad F, Taplin ME, Sternberg CN, Miller K, de WR, Mulders P, Chi KN, Shore ND, Armstrong AJ, Flaig TW, Flechon A, Mainwaring P, Fleming M, Hainsworth JD, Hirmand M, Selby B, Seely L, de Bono JS. Increased survival with enzalutamide in prostate cancer after chemotherapy. N Engl J Med 2012;367:1187–1197.
5. Fizazi K, Scher HI, Molina A, Logothetis CJ, Chi KN, Jones RJ, Staffurth JN, North S, Vogelzang NJ, Saad F, Mainwaring P, Harland S, Goodman OB Jr., Sternberg CN, Li JH, Kheoh T, Haqq CM, de Bono JS. Abiraterone acetate for treatment of metastatic castration-resistant prostate cancer: Final overall survival analysis of the COU-AA-301 randomised, double-blind, placebo-controlled phase 3 study. Lancet Oncol 2012;13:983–992.
6. Berthold DR, Pond GR, Soban F, de WR, Eisenberger M, Tannock IF. Docetaxel plus prednisone or mitoxantrone plus prednisone for advanced prostate cancer: Updated survival in the TAX 327 study. J Clin Oncol 2008;26: 242–245.
7. Petrylak DP, Tangen CM, Hussain MH, Lara PN, Jr., Jones JA, Taplin ME, Burch PA, Berry D, Moinpour C, Kohli M, Benson MC, Small EJ, Raghavan D, Crawford ED. Docetaxel and estramustine compared with mitoxantrone and prednisone for advanced refractory prostate cancer. N Engl J Med 2004; 351:1513–1520.

8. Drost J, Karthaus WR, Gao D, Driehuis E, Sawyers CL, Chen Y, Clevers H. Organoid culture systems for prostate epithelial and cancer tissue. Nat Protoc 2016;11:347–358.
9. Gao D, Chen Y. Organoid development in cancer genome discovery. Curr Opin Genet Dev 2015;30:42–48.
10. Tentler JJ, Tan AC, Weekes CD, Jimeno A, Leong S, Pitts TM, Arcaroli JJ, Messersmith WA, Eckhardt SG. Patient-derived tumour xenografts as models for oncology drug development. Nat Rev Clin Oncol 2012;9:338–350.
11. Daniel VC, Marchionni L, Hierman JS, Rhodes JT, Devereux WL, Rudin CM, Yung R, Parmigiani G, Dorsch M, Peacock CD, Watkins DN. A primary xenograft model of small-cell lung cancer reveals irreversible changes in gene expression imposed by culture in vitro. Cancer Res 2009;69:3364–3373.
12. Kopetz S, Lemos R, Powis G. The promise of patient-derived xenografts: The best laid plans of mice and men. Clin Cancer Res 2012;18:5160–5162.
13. Gao H, Korn JM, Ferretti S, Monahan JE, Wang Y, Singh M, Zhang C, Schnell C, Yang G, Zhang Y, Balbin OA, Barbe S, Cai H, Casey F, Chatterjee S, Chiang DY, Chuai S, Cogan SM, Collins SD, Dammassa E, Ebel N, Embry M, Green J, Kauffmann A, Kowal C, Leary RJ, Lehar J, Liang Y, Loo A, Lorenzana E, Robert ME, III, McLaughlin ME, Merkin J, Meyer R, Naylor TL, Patawaran M, Reddy A, Roelli C, Ruddy DA, Salangsang F, Santacroce F, Singh AP, Tang Y, Tinetto W, Tobler S, Velazquez R, Venkatesan K, Von AF, Wang HQ, Wang Z, Wiesmann M, Wyss D, Xu F, Bitter H, Atadja P, Lees E, Hofmann F, Li E, Keen N, Cozens R, Jensen MR, Pryer NK, Williams JA, Sellers WR. High-throughput screening using patient-derived tumor xenografts to predict clinical trial drug response. Nat Med 2015;21:1318–1325.
14. Townsend EC, Murakami MA, Christodoulou A, Christie AL, Koster J, DeSouza TA, Morgan EA, Kallgren SP, Liu H, Wu SC, Plana O, Montero J, Stevenson KE, Rao P, Vadhi R, Andreeff M, Armand P, Ballen KK, Barzaghi-Rinaudo P, Cahill S, Clark RA, Cooke VG, Davids MS, DeAngelo DJ, Dorfman DM, Eaton H, Ebert BL, Etchin J, Firestone B, Fisher DC, Freedman AS, Galinsky IA, Gao H, Garcia JS, Garnache-Ottou F, Graubert TA, Gutierrez A, Halilovic E, Harris MH, Herbert ZT, Horwitz SM, Inghirami G, Intlekoffer AM, Ito M, Izraeli S, Jacobsen ED, Jacobson CA, Jeay S, Jeremias I, Kelliher MA, Koch R, Konopleva M, Kopp N, Kornblau SM, Kung AL, Kupper TS, LaBoeuf N, LaCasce AS, Lees E, Li LS, Look AT, Murakami M, Muschen M, Neuberg D, Ng SY, Odejide OO, Orkin SH, Paquette RR, Place AE, Roderick JE, Ryan JA, Sallan SE, Shoji B, Silverman LB, Soiffer RJ, Steensma DP, Stegmaier K, Stone RM, Tamburini J, Thorner AR, van HP, Wadleigh M, Wiesmann M, Weng AP, Wuerthner JU, Williams DA, Wollison BM, Lane AA, Letai A, Bertagnolli MM, Ritz J, Brown M, Long H, Aster JC, Shipp MA, Griffin JD, Weinstock DM. The public repository of xenografts enables discovery and randomized phase II-like trials in mice. Cancer Cell 2016;29:574–586.
15. Bertotti A, Papp E, Jones S, Adleff V, Anagnostou V, Lupo B, Sausen M, Phallen J, Hruban CA, Tokheim C, Niknafs N, Nesselbush M, Lytle K, Sassi F, Cottino F, Migliardi G, Zanella ER, Ribero D, Russolillo N, Mellano A, Muratore A, Paraluppi G, Salizzoni M, Marsoni S, Kragh M, Lantto J, Cassingena A, Li QK, Karchin R, Scharpf R, Sartore-Bianchi A, Siena S, Diaz LA, Jr., Trusolino L, Velculescu VE. The genomic landscape of response to EGFR blockade in colorectal cancer. Nature 2015;526:263–267.
16. Kumar A, Coleman I, Morrissey C, Zhang X, True LD, Gulati R, Etzioni R, Bolouri H, Montgomery B, White T, Lucas JM, Brown LG, Dumpit RF, DeSarkar N, Higano C, Yu EY, Coleman R, Schultz N, Fang M, Lange PH, Shendure J, Vessella RL, Nelson PS. Substantial interindividual and limited intraindividual genomic diversity among tumors from men with metastatic prostate cancer. Nat Med 2016;22:369–378.
17. Weaver AN, Cooper TS, Rodriguez M, Trummell HQ, Bonner JA, Rosenthal EL, Yang ES. DNA double strand break repair defect and sensitivity to poly ADP-ribose polymerase (PARP) inhibition in human papillomavirus 16-positive head and neck squamous cell carcinoma. Oncotarget 2015;6:26995–27007.
18. True LD, Buhler KR, Quinn J, Ellis WJ, Nelson P, Clegg N, Macoska JA, Norwood T, Liu A, Ellis W, Lange PH, Vessella R. A neuroendocrine/small cell prostate carcinoma xenograft: LuCaP 49. Am J Pathol 2002;161:705–715.
19. Ellis WJ, Vessella RL, Buhler KR, Bladou F, True LD, Bigler SA, Curtis D, Lange PH. Characterization of a novel androgen-sensitive, prostate-specific antigen-producing prostatic carcinoma xenograft: LuCaP 23. Clin Cancer Res 1996;2:1039–1048.
20. Montgomery B, Nelson PS, Vessella R, Kalhorn T, Hess D, Corey E. Estradiol suppresses tissue androgens and prostate cancer growth in castration resistant prostate cancer. BMC Cancer 2010;10:244.
21. Nguyen HM, Ruppender N, Zhang X, Brown LG, Gross TS, Morrissey C, Gulati R, Vessella RL, Schimmoller F, Aftab DT, Corey E. Cabozantinib inhibits growth of androgen-sensitive and castration-resistant prostate cancer and affects bone remodeling. PLoS ONE 2013;8:e78881.
22. Mostaghel EA, Marck BT, Plymate SR, Vessella RL, Balk S, Matsumoto AM, Nelson PS, Montgomery RB. Resistance to CYP17A1 inhibition with abiraterone in castration-resistant prostate cancer: Induction of steroidogenesis and androgen receptor splice variants. Clin Cancer Res 2011;17:5913–5925.
23. Holcomb IN, Young JM, Coleman IM, Salari K, Grove DI, Hsu L, True LD, Roudier MP, Morrissey CM, Higano CS, Nelson PS, Vessella RL, Trask BJ. Comparative analyses of chromosome alterations in soft-tissue metastases within and across patients with castration-resistant prostate cancer. Cancer Res 2009;69:7793–7802.
24. Zhang X, Coleman IM, Brown LG, True LD, Kollath L, Lucas JM, Lam HM, Dumpit R, Corey E, Chery L, Lakely B, Higano CS, Montgomery B, Roudier M, Lange PH, Nelson PS, Vessella RL, Morrissey C. SRRM4 expression and the loss of REST activity may promote the emergence of the neuroendocrine phenotype in castration-resistant prostate cancer. Clin Cancer Res 2015;21:4698–4708.
25. Kalhorn TF, Page ST, Howald WN, Mostaghel EA, Nelson PS. Analysis of testosterone and dihydrotestosterone from biological fluids as the oxime derivatives using high-performance liquid chromatography/tandem mass spectrometry. Rapid Commun Mass Spectrom 2007;21:3200–3206.
26. Corey E, Quinn JE, Bladou F, Brown LG, Roudier MP, Brown JM, Buhler KR, Vessella RL. Establishment and characterization of osseous prostate cancer models: Intra-tibial injection of human prostate cancer cells. Prostate 2002;52:20–33.
27. Brubaker KD, Vessella RL, True LD, Thomas R, Corey E. Cathepsin K mRNA and protein expression in prostate cancer progression. J Bone Miner Res 2003;18:222–230.
28. Michiel Sedelaar JP, Dalrymple SS, Isaacs JT. Of mice and men–warning: Intact versus castrated adult male mice as xenograft hosts are equivalent to hypogonadal versus abiraterone treated aging human males, respectively. Prostate 2013;73:1316–1325.

29. Robinson D, Van Allen EM, Wu YM, Schultz N, Lonigro RJ, Mosquera JM, Montgomery B, Taplin ME, Pritchard CC, Attard G, Beltran H, Abida W, Bradley RK, Vinson J, Cao X, Vats P, Kunju LP, Hussain M, Feng FY, Tomlins SA, Cooney KA, Smith DC, Brennan C, Siddiqui J, Mehra R, Chen Y, Rathkopf DE, Morris MJ, Solomon SB, Durack JC, Reuter VE, Gopalan A, Gao J, Loda M, Lis RT, Bowden M, Balk SP, Gaviola G, Sougnez C, Gupta M, Yu EY, Mostaghel EA, Cheng HH, Mulcahy H, True LD, Plymate SR, Dvinge H, Ferraldeschi R, Flohr P, Miranda S, Zafeiriou Z, Tunariu N, Mateo J, Perez-Lopez R, Demichelis F, Robinson BD, Schiffman M, Nanus DM, Tagawa ST, Sigaras A, Eng KW, Elemento O, Sboner A, Heath EI, Scher HI, Pienta KJ, Kantoff P, de Bono JS, Rubin MA, Nelson PS, Garraway LA, Sawyers CL, Chinnaiyan AM. Integrative clinical genomics of advanced prostate cancer. Cell 2015;161:1215–1228.

30. Boyd LK, Mao X, Lu YJ. The complexity of prostate cancer: Genomic alterations and heterogeneity. Nat Rev Urol 2012;9: 652–664.

31. Pritchard CC, Morrissey C, Kumar A, Zhang X, Smith C, Coleman I, Salipante SJ, Milbank J, Yu M, Grady WM, Tait JF, Corey E, Vessella RL, Walsh T, Shendure J. Nelson PS. Complex MSH2 and MSH6 mutations in hypermutated microsatellite unstable advanced prostate cancer. Nat Commun 2014;5:4988.

32. Tan J, Sharief Y, Hamil KG, Gregory CW, Zang DY, Sar M, Gumerlock PH, deVere White RW, Pretlow TG, Harris SE, Wilson EM, Mohler JL, French FS. Dehydroepiandrosterone activates mutant androgen receptors expressed in the androgen-dependent human prostate cancer xenograft CWR22 and LNCaP cells. Mol Endocrinol 1997;11:450–459.

33. Gottlieb B, Beitel LK, Nadarajah A, Paliouras M, Trifiro M. The androgen receptor gene mutations database: 2012 update. Hum Mutat 2012(33):887–894.

34. Sun S, Sprenger CC, Vessella RL, Haugk K, Soriano K, Mostaghel EA, Page ST, Coleman IM, Nguyen HM, Sun H, Nelson PS, Plymate SR. Castration resistance in human prostate cancer is conferred by a frequently occurring androgen receptor splice variant. J Clin Invest 2010;120:2715–2730.

35. Antonarakis ES, Lu C, Wang H, Luber B, Nakazawa M, Roeser JC, Chen Y, Mohammad TA, Chen Y, Fedor HL, Lotan TL, Zheng Q, De Marzo AM, Isaacs JT, Isaacs WB, Nadal R, Paller CJ, Denmeade SR, Carducci MA, Eisenberger MA, Luo J. AR-V7 and resistance to enzalutamide and abiraterone in prostate cancer. N Engl J Med 2014;371:1028–1038.

36. Antonarakis ES, Armstrong AJ, Dehm SM, Luo J. Androgen receptor variant-driven prostate cancer: Clinical implications and therapeutic targeting. Prostate Cancer Prostatic Dis 2016; 19:231–241.

37. Montgomery RB, Mostaghel EA, Vessella R, Hess DL, Kalhorn TF, Higano CS, True LD, Nelson PS. Maintenance of intratumoral androgens in metastatic prostate cancer: A mechanism for castration-resistant tumor growth. Cancer Res 2008;68: 4447–4454.

38. Kumar A, White TA, MacKenzie AP, Clegg N, Lee C, Dumpit RF, Coleman I, Ng SB, Salipante SJ, Rieder MJ, Nickerson DA, Corey E, Lange PH, Morrissey C, Vessella RL, Nelson PS, Shendure J. Exome sequencing identifies a spectrum of mutation frequencies in advanced and lethal prostate cancers. Proc Natl Acad Sci USA 2011;108:17087–17092.

39. Thadani-Mulero M, Portella L, Sun S, Sung M, Matov A, Vessella RL, Corey E, Nanus DM, Plymate SR, Giannakakou P. Androgen receptor splice variants determine taxane sensitivity in prostate cancer. Cancer Res 2014;74:2270–2282.

40. Diamond E, Garcias MC, Karir B, Tagawa ST. The evolving role of cytotoxic chemotherapy in the management of patients with metastatic prostate cancer. Curr Treat Options Oncol 2015;16:9.

41. Corey E, Quinn JE, Vessella RL. A novel method of generating prostate cancer metastases from orthotopic implants. Prostate 2003;56:110–114.

42. Pritchard CC, Mateo J, Walsh MF, De SN, Abida W, Beltran H, Garofalo A, Gulati R, Carreira S, Eeles R, Elemento O, Rubin MA, Robinson D, Lonigro R, Hussain M, Chinnaiyan A, Vinson J, Filipenko J, Garraway L, Taplin ME, AlDubayan S, Han GC, Beightol M, Morrissey C, Nghiem B, Cheng HH, Montgomery B, Walsh T, Casadei S, Berger M, Zhang L, Zehir A, Vijai J, Scher HI, Sawyers C, Schultz N, Kantoff PW, Solit D, Robson M, Van Allen EM, Offit K, de BJ, Nelson PS. Inherited DNA-Repair gene mutations in men with metastatic prostate cancer. N Engl J Med 2016;375:443–453.

43. Roudier MP, Vesselle H, True LD, Higano CS, Ott SM, King SH, Vessella RL. Bone histology at autopsy and matched bone scintigraphy findings in patients with hormone refractory prostate cancer: The effect of bisphosphonate therapy on bone scintigraphy results. Clin Exp Metastasis 2003;20:171–180.

44. Roudier MP, True LD, Higano CS, Vesselle H, Ellis WJ, Lange PH, Vessella RL. Phenotypic heterogeneity of androgen-Independent prostate cancer bone metastases. Hum Pathol 2003;34: 646–653.

45. Chen CD, Welsbie DS, Tran C, Baek SH, Chen R, Vessella R, Rosenfeld MG, Sawyers CL. Molecular determinants of resistance to antiandrogen therapy. Nat Med 2004;10:33–39.

46. Beer TM, Armstrong AJ, Rathkopf D, Loriot Y, Sternberg CN, Higano CS, Iversen P, Evans CP, Kim CS, Kimura G, Miller K, Saad F, Bjartell AS, Borre M, Mulders P, Tammela TL, Parli T, Sari S, van OS, Theeuwes A, Tombal B. Enzalutamide in men with chemotherapy-naive metastatic castration-resistant prostate cancer: Extended analysis of the phase 3 PREVAIL study. Eur Urol 2016.

47. Zhang X, Morrissey C, Sun S, Ketchandji M, Nelson PS, True LD, Vakar-Lopez F, Vessella RL, Plymate SR. Androgen receptor variants occur frequently in castration resistant prostate cancer metastases. PLoS One 2011;6:e27970.

48. Myung JK, Banuelos CA, Fernandez JG, Mawji NR, Wang J, Tien AH, Yang YC, Tavakoli I, Haile S, Watt K, McEwan IJ, Plymate S, Andersen RJ, Sadar MD. An androgen receptor N-terminal domain antagonist for treating prostate cancer. J Clin Invest 2013;123:2948–2960.

SUPPORTING INFORMATION

Additional supporting information may be found in the online version of this article at the publisher's web-site.